ELSEVIER

Journal of Chromatography A, 828 (1998) 19–35

JOURNAL OF CHROMATOGRAPHY A

Theoretical analysis of the behavior of a centrally injected band in a homogeneous chromatographic column

Tong Yun[1,a,b], Maureen S. Smith[a,b], Georges Guiochon[a,b,*]

[a]*Department of Chemistry, University of Tennessee, Knoxville, TN 37996-1600, USA*

[b]*Division of Chemical and Analytical Sciences, Oak Ridge National Laboratory, Oak Ridge, TN 37831-6120, USA*

Abstract

A new implementation of the equilibrium–dispersive model permits the study of problems requiring two-space dimensions for their modeling, such as a nonhomogeneous column with a cylindrical symmetry, a nonplanar injection with a cylindrical symmetry, or a cylindrical central injection. The migration and broadening of a cylindrical band coaxial with the column but narrower, moving along a homogeneous column is studied. The axial and radial profiles of the band inside the column and the elution profiles are calculated. These profiles depend on both the radial and the axial dispersion coefficients. The radial dispersion coefficient decreases with increasing mobile phase velocity and is usually low, much lower than the axial dispersion coefficient. Thus, the material in a relatively wide central injection made on a wide bore column may never have a chance to get close to the column wall. The clearance required at injection is estimated.

Keywords: Equilibrium–dispersive model; Band profiles; Preparative chromatography; Injection parameters

1. Introduction

Actual chromatographic columns are not entirely homogeneous as has been postulated in almost all theoretical studies undergone so far on the migration and broadening of band profiles under linear or nonlinear conditions [1]. Various experimental results [2–14] have shown that, in most cases, the packing density and the permeability of a column are different in the central core region of the packing and along the column wall. A zone of packing along this wall seems to have properties which are markedly different from those of the column core. The radial distribution of the column properties (e.g., of the local mobile phase velocity) affects considerably band propagation and band broadening. So, if a zone injected centrally does not spread sufficiently in the radial direction for any significant amount of solute to interact with the wall region, its behavior will depend only on the properties of the homogeneous core region and the column efficiency could be excellent [2–9]. By contrast, if the zone penetrates inside the wall region, the difference in migration properties between wall region and the core results in poor column performance. Results obtained with wide [2–4] and narrow [5–7] analytical columns tend to suggest that the wall region has a nearly constant thickness, when expressed in average particle diameters. However, more recent data obtained with preparative columns [8,9] show quite a different picture. The thickness of the ''wall layer'' increases

*Corresponding author. Address for correspondence: Department of Chemistry, 575 Buehler Hall, University of Tennessee, Knoxville, TN 37996-1600, USA.

[1]Present address: Chiral Technologies Inc., Exton, PA, USA.

0021-9673/98/$ – see front matter
PII: S0021-9673(98)00663-3

with increasing column diameter and depends on the packing procedure used. Data are still lacking on actual preparative columns and we do not know whether a proportionality relationship applies. Furthermore, the mechanism through which this radial layering occurs is still unknown, although it is now established that this has much to do with friction of the bed of packing material against the column wall [14–16].

Bands do disperse at different rates, following different mechanisms in the axial and the radial directions, as first demonstrated by Knox and coworkers [2,3] and by Eon [4]. Their results have been confirmed by recent, systematic determinations by pulsed field gradient (PFG) nuclear magnetic resonance (NMR) of the axial and transverse dispersion coefficients in a 25 mm I.D. column, as a function of the mobile phase velocity [10–12]. A high coefficient of radial dispersion would help in keeping the band profile flat and narrow in the direction of the column axis, in spite of local inhomogeneities of the packing. However, radial dispersion is slow, dispersion is an inefficient mass transfer process over long distances, and there does not seem to exist any methods to accelerate it. On the contrary, preparative chromatography tends to be carried out at relatively high mobile phase flow velocities [1], at which the axial height equivalent to a theoretical plate (HETP) is higher than the minimum, while the transverse dispersion coefficient, which decreases monotonically with increasing flow velocity [10–12], is at least several times lower.

Thus, it appears potentially attractive to proceed to a centrally located injection, provided that only a narrow annulus along the column wall would be kept free of sample, a thin sheath of pure liquid phase being pumped along the wall, at the column inlet, during the feed injection [3]. Besides the conventional width or duration of the injection, we introduce a second parameter, its radial width, or ratio of the radius of the injected band to the column radius (Fig. 1). The zone would interact only with the most homogeneous region of the packing, providing a better resolution between the separated bands [9]. The thickness of the sheath should be of the same order as the thickness of the heterogeneous wall region. Depending on the homogeneity of the column bed, this wall layer varies from a few percent to

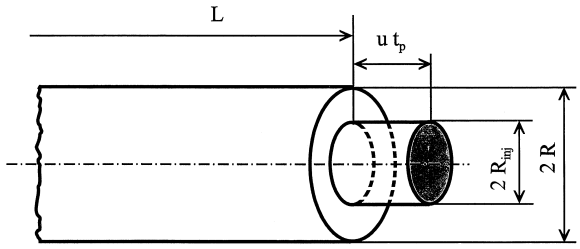

Fig. 1. Representation of the profile of the injection band. Duration t_p, radius R_{inj}, length ut_p in the mobile phase just upstream the column inlet. Depending on the case, the central injection area is 0.01, 25, 50, or 80% of the total column cross-sectional area. In all cases, the loading factor is 10% based on mass of stationary phase in a column of length L and radius R_{inj}. The column length is 15 cm, its radius, 5 cm, with an aspect ratio of 3. $Pe_a = 2000$.

20–25% of the column radius [6–9]. If we keep constant the concentration of the injected sample, in order to keep constant the local degree of overloading of the stationary phase in its core region, the high values would result in a considerable decrease of the sample size at a given degree of column overloading. While the increased resolution between bands would be important, allowing a significant increase in the column overload, it is probable that the balance between all these changes would bring a loss of production rate, possibly an unacceptable one. The low value of the sheath thickness would result in a relatively small loss of production rate for a marked increase in the resolution, and a possibly attractive compromise, allowing the production of purer fractions with a higher recovery yield (at constant degree of column overloading) or a higher production rate (at constant band resolution).

The experimental investigation of this approach to determine the optimum sheath thickness and loading factor will be time consuming and expensive because wide bore columns, of at least 10 to 15 cm in diameter, must be used to acquire meaningful information. Before undertaking such a study, it is useful to calculate the broad lines of a possible compromise. For this purpose, we need first to solve two different problems. First, we must calculate the migration of a centrally injected band in a homogeneous column and its broadening in the axial and radial directions. Second, we must calculate the influence that a thin layer of packing against the

column wall, with properties (e.g., apparent density, permeability, flow velocity, apparent axial dispersion coefficient) different from those of the core region may have on the apparent performance of the column. The solutions of these two problems require a program implementing the numerical integration of the mass balance equation of the equilibrium–dispersive model of chromatography in three dimensions, the two-dimensional space (z, r) of a cylindrical column and time. We have recently developed such a program [17,18]. The solution of the second problem requires, in addition, the modeling of the physical structure of the wall region, as opposed to the core region of the column. The systematic and abundant experimental data required to discuss this issue are beginning to be available [14]. We report here on the solution of the first of these problems, on the broadening of centrally injected bands.

2. Theory

We first recall briefly the fundamental characteristics of the equilibrium–dispersive model [1], then discuss in detail the changes that must be made properly to model either a cylindrical, heterogeneous column [17] or the migration of an injected pulse which has a rectangular profile along the column axis, is coaxial to the column (assumed to be homogeneous in this work) but has a diameter smaller than the column. The profile of this injection is represented in Fig. 1.

2.1. The equilibrium–dispersive model

The equilibrium–dispersive model assumes that mass transfer across the column is instantaneous and that the mobile and stationary phases at any point in the column are constantly in equilibrium [1]. The actual influence of the mass transfer resistances, which are never negligible, is taken into account by including it with axial diffusion into an apparent axial dispersion term. Thus, in this model, the apparent axial dispersion coefficient includes contributions for axial diffusion, eddy diffusion and the mass transfer resistances. We give only a brief summary of the characteristic features of this model, for the sake of comparison. The mass balance equation of the equilibrium–dispersive model for a linear column is written

$$\frac{\partial C}{\partial t} + F \cdot \frac{\partial q}{\partial t} + u \cdot \frac{\partial C}{\partial z} = D_a \frac{\partial^2 C}{\partial z^2} \quad (1)$$

where C and q are the solute concentrations in the mobile and stationary phase, respectively, t is the time, z is the distance along the column, F is the phase ratio ($F=(1-\varepsilon)/\varepsilon$, with ε, total column porosity), u is the mobile phase flow velocity, and D_a is the apparent dispersion coefficient [1]. The relationship between the apparent dispersion coefficient and the column HETP under linear conditions is given by

$$H_a = \frac{2D_a}{u} \quad (2)$$

Since the equilibrium–dispersive model assumes that the mobile and stationary phases are in equilibrium everywhere in the column, at any time, the concentrations q and C in Eq. (1) are related by the isotherm equation. Usually, a Langmuir isotherm model is assumed in theoretical works such as the present one

$$q = \frac{aC}{1+bC} \quad (3)$$

where a and b are numerical coefficients.

The initial and boundary conditions used are those of elution chromatography. Initially, the column is percolated by a stream of pure mobile phase in equilibrium with the stationary phase, with no solute present. A pulse of solute of defined profile, usually a rectangular pulse of height C_0 and width t_p is injected, beginning at the origin of time.

2.2. The mathematical model of a cylindrical column

The simplest deviation from a homogeneous column with a flat injection band is a column having a cylindrical symmetry. In this case, the concentration distribution at a given time of a band migrating along the column depends on the position, z, and the distance, r, from the column axis. It does not depend on the azimuthal angle around the column axis. The differential element of the column is a ring of axial

thickness dz, limited by the cylinders of radii r and $r+\mathrm{d}r$. In this element, the mass balance is written

$$\frac{\partial C}{\partial t}+F\cdot\frac{\partial q}{\partial t}+u\cdot\frac{\partial C}{\partial z}=D_{\mathrm{a}}\cdot\frac{\partial^2 C}{\partial z^2}+\frac{D_{\mathrm{r}}}{r}\cdot\frac{\partial\left(r\dfrac{\partial C}{\partial r}\right)}{\partial r} \tag{4}$$

where D_{r} is the radial dispersion coefficient, related to the radial plate height by

$$H_{\mathrm{r}}=\frac{2D_{\mathrm{r}}}{u} \tag{5}$$

The axial plate height is still related to the apparent axial dispersion coefficient by Eq. (2).

Although, in the general case, D_{a} and D_{r} could both be functions of the coordinates z and r and of the concentration, we assumed in writing Eq. (4) that they are constant. We will also assume in this work that the column itself is homogeneous. Accordingly, we will not encounter the difficulties found in a previous work [17] regarding the assumption that there is no convective transport in the radial direction of the column. Since the column is supposed to be homogeneous, there are no radial variations of the packing density, hence the column porosity, its permeability, and the retention factors are constant throughout the bed. Streamlines remain parallel to the column axis. With a homogeneous column, the need to consider the radial dimension arises from the use of a boundary condition that is a function of the radial position.

The presentation of numerical solutions of Eq. (4) and their discussion are greatly simplified if some reduced variables are introduced at this stage. These are the reduced axial position (χ), the reduced column radius (ρ), the reduced time (τ), the axial ($\mathrm{Pe_a}$) and radial ($\mathrm{Pe_r}$) column Peclet numbers (note that these two Peclet numbers are different from the conventional particle Peclet number or reduced velocity, $\nu=ud_{\mathrm{p}}/D_{\mathrm{m}}$), and the column aspect ratio (Φ) which are defined as follows

$$\chi=\frac{z}{L} \tag{6a}$$

$$\rho=\frac{r}{R} \tag{6b}$$

$$\tau=\frac{ut}{L} \tag{6c}$$

$$\mathrm{Pe_a}=\frac{uL}{D_{\mathrm{a}}}=2\cdot\frac{L}{H_{\mathrm{a}}} \tag{6d}$$

$$\mathrm{Pe_r}=\frac{uL}{D_{\mathrm{r}}}=2\cdot\frac{L}{H_{\mathrm{r}}} \tag{6e}$$

$$\Phi=\frac{L}{R} \tag{6f}$$

where L is the column length and R its radius. Combination of Eqs. (4), (6a)–(6f) gives the mass balance equation in reduced coordinates:

$$\frac{\partial C}{\partial\tau}+F\cdot\frac{\partial q}{\partial\tau}+\frac{\partial C}{\partial\chi}=\frac{1}{\mathrm{Pe_a}}\cdot\frac{\partial^2 C}{\partial\chi^2}+\frac{\Phi}{\mathrm{Pe_r}}\cdot\frac{\partial\left(\rho\dfrac{\partial C}{\partial\rho}\right)}{\partial\rho} \tag{7}$$

There are four parameters in this equation, F, $\mathrm{Pe_a}$, $\mathrm{Pe_r}$ and Φ. In practice, it is extremely difficult, if not impossible, to adjust the first one, F, which is mostly a property of the packing material and its internal porosity. However, F depends on the packing density, through the external porosity or fraction of the column volume available to the stream of mobile phase percolating through the column packing. Recent results have shown that the packing density depends somewhat on the stress applied to the column packing during the preparation of the column [14,19]. Still, it does not seem possible to use an adjustable external stress to modify significantly, at will, the column properties. By contrast, the other three parameters are easily adjustable. Note that both D_{a} (Eq. (2)) and D_{r} (Eq. (5)) are functions of the flow velocity through the corresponding plate height equation. Thus, the Peclet number ratio, $\mathrm{Pe_a}/\mathrm{Pe_r}$, does not remain constant when this velocity is changed.

The initial condition of the elution problem is a column under hydrodynamic steady-state, with the mobile and stationary phase in thermodynamic equilibrium, but empty of sample

$$C(x,\,t=0)=0\quad 0\le x\le L \tag{8}$$

For a central injection, coaxial with the column, the boundary condition in the axial direction is the injection of a rectangular pulse of duration t_{p} in the

central area of the column, with a radius R_{inj} ($R_{inj} < R$). The condition is written as follows

$$C(x=0, t) = C_0 \quad 0 \le r \le R_{inj} \quad 0 \le t \le t_p \tag{9a}$$

$$C(x=0, t) = 0 \quad R_{inj} < r \le R \quad 0 \le t \le t_p \tag{9b}$$

$$C(x=0, t) = 0 \quad t < 0 \quad t > t_p \tag{9c}$$

where C_0 is the initial concentration of the solute in the sample. Thus, the injected amount is $n = C_0 t_p F_v R_{inj}^2 / R^2$ (a number of moles), where F_v is the mobile phase flow-rate. The loading factor density along the column axis is $L_f = u t_p C^0 / [L(1-\varepsilon) q_s]$. The degree of overloading of the phase system does not depend on R_{inj} as long as the concentration in the center of the band is not affected (see later discussion).

There are also two boundary conditions in the radial direction. They state that (i) no concentration can penetrate inside the column wall and (ii) the concentration distribution is symmetrical around the column axis, i.e., that the radial gradient of concentration is 0 at the wall (i) and at the column axis (ii). Hence

$$\frac{\partial C}{\partial \rho} = 0 \quad \text{for } r = R \tag{10a}$$

$$\frac{\partial C}{\partial \rho} = 0 \quad \text{for } r = 0 \tag{10b}$$

The system of equations just described has no analytical solution. Numerical solutions can be calculated using a suitable program [17,18].

2.3. Special cases

There are two special cases to consider for the system of Eqs. (4), (5), (6a)–(6f), (7), (8), (9a)–(9c) because they have been discussed previously in the literature. They are the cases in which there is no retention, i.e., when $q \equiv 0 \forall C$, and in which the equilibrium isotherm is linear (i.e., $q = aC$).

2.3.1. No retention

If there is no retention, Eq. (4) simplifies into

$$\frac{\partial C}{\partial t} + u \cdot \frac{\partial C}{\partial z} = D_a \cdot \frac{\partial^2 C}{\partial z^2} + \frac{D_r}{r} \cdot \frac{\partial \left(r \frac{\partial C}{\partial r} \right)}{\partial r} \tag{11}$$

This equation describes the migration of a centrally injected band of a nonretained component along the column. The initial and boundary conditions remain the same (Eqs. (8), (9a)–(9c), (10a), (10b)). Eq. (11) has been studied by Klinkenberg et al. [20] with different boundary conditions, corresponding to a constant flow-rate in a cylindrical tube (Hagen–Poiseuille profile) with a local source of concentration C in a point of the column axis. Thus, the analytical solution derived is of limited use in the chromatographic problem which has an entirely different boundary condition (flat velocity profile, finite width of the injection source, pulse injection).

Eq. (11) was also studied by Gunn [21] who derived an analytical solution for a set of boundary conditions similar to those corresponding to our problem. Gunn considered the same problem as ours, for a radially heterogeneous packed column. However, he was not interested in chromatography and assumed that there was no retention. At a time when there were no computers, he simplified the problem by considering a homogeneous core layer and a homogeneous wall layer, the two layer having different properties (cross-section areas, permeabilities, coefficients of axial dispersion, velocities). This model is similar to a wall-coated open tubular column (i.e., a Golay column) in liquid chromatography, except that the mobile phase flows also, although at a lower velocity, in the layer of stationary phase, along the column wall. This is not a sufficiently realistic model for our purpose.

Finally, Eon [4] adapted the solution of Klinkenberg et al. [20] to the chromatographic problem, solving Eq. (4) for different boundary conditions, not explicitly stated but which seem to correspond to the injection of a centrally located δ^2 pulse, infinitely short in injection time and infinitely narrow in radius but containing a finite amount of material. The radial distribution of the concentration at the column exit, when the maximum of the band is being eluted (i.e., ''when half the peak has left the column'' [4]), was calculated for columns of different lengths. In the results reported, the column length was scaled by the length, L_1, for which the peak variance (in the radial

direction) is one-quarter of the column radius. It is easy to show that this distance is given by

$$L_1 = \frac{R^2}{d_p} \cdot \frac{1}{16h_r} = \frac{R^2}{d_p} \cdot \frac{1}{16(2\gamma/\nu + D)} \quad (12a)$$

$$= \frac{R}{4}\sqrt{\frac{Pe_r}{2}} \quad (12b)$$

Eq. (12a) was derived by Eon [4]; it is equivalent to Eq. (12b) with our definitions. Obviously, for a column length equal to L_1, the radial distribution of concentration at elution is practically identical to a Gaussian curve having a standard deviation equal to one-quarter of the column radius (at the column wall, i.e., at four standard deviations from the apex, the relative height of a Gaussian profile is $3.4 \cdot 10^{-4}$ so the presence of the wall causes only a negligible perturbation anywhere, except in its immediate proximity). The presence of the wall begins to affect the radial profile for column lengths between $2L_1$ and $4L_1$ [4]. Note, however, that we are interested here in the injection of bands which have a wide rectangular profile, both in the time and the radial dimensions. Accordingly, the radial profile of the band will be affected for lengths shorter than L_1. So, we cannot use this analytical solution and must calculate numerical solutions.

2.3.2. Linear isotherm

In this case, the isotherm is written: $q = aC$ and the mass balance equation (Eq. (4)) simplifies to

$$(1 + Fa) \cdot \frac{\partial C}{\partial t} + u \cdot \frac{\partial C}{\partial z} = D_a \cdot \frac{\partial^2 C}{\partial z^2} + \frac{D_r}{\rho} \cdot \frac{\partial\left(\rho \frac{\partial C}{\partial \rho}\right)}{\partial \rho} \quad (13)$$

Eq. (13) is very similar to Eq. (11) because $(1+Fa)$ is a constant. The solutions obtained for Eq. (11) can easily be extended to Eq. (13).

2.4. Numerical algorithm and calculations

The model described by Eq. (4) and an isotherm model such as Eq. (3) is an extension of the conventional equilibrium–dispersive model (Eq. (1)) to problems with two space-dimensions, e.g., to the case of a column with cylindrical symmetry. It has no analytical solution but it is possible to write simple computational schemes for the calculation of its numerical solutions, using finite difference algorithms [1].

In the case in which only one-space dimension is considered, the forward–backward numerical scheme has, over alternative ones, the advantage of being much faster. In this scheme, there is a simple relationship between the time and space integration increments and the apparent axial dispersion coefficient or the axial HETP of the column. With the forward–backward numerical scheme, for example, the calculation of numerical solutions of the ideal model ($D_a = 0$ in Eq. (1)) should be carried out with increments equal to

$$\delta z = \frac{H_a}{A - 1} \quad (14a)$$

$$\delta t = \frac{aH_a}{A - 1} \cdot \frac{1 + k_0'}{u} \quad (14b)$$

where A is the Courant number of the problem, $A = u\delta t/(1 + k_0')\delta_z$, which must be larger than 1 with this calculation scheme [1]. This calculation method proves to be extremely fast and the solutions obtained are in excellent agreement with those given by more conventional methods [1]. This makes the approach most attractive for the numerical calculation of solutions of Eq. (4), a calculation which is much longer since the problem has now one more space dimension. Thus, a finite difference algorithm based on the same principles as the forward–backward scheme used with columns having a single space dimension, was developed and programmed. The details of this program are discussed elsewhere [17,18].

Several series of numerical calculations have been done to illustrate the influence of the main parameters, the radial dispersion characterized by Pe_r, the aspect ratio ($\Phi = L/R$), and the relative width of the injection, R_{inj}/R. The latter is represented by three groups of calculations. The first two groups, with values of the relative width of 0.010 and 0.50, corresponding to fractions $(R_{inj}/R)^2$ of the maximum possible feed amount (cross-section injection) of 0.01% and 25%, respectively, correspond to elutions under infinite column diameter conditions. The third group includes injections with relative width of 0.70

and 0.90 (relative amounts, 0.50 and 0.80, respectively) that give bands which eventually interact with the wall before their elution. Obviously, these results depend much on the values of the other two main parameters, the aspect ratio and the radial Peclet number.

2.5. Infinite column diameter conditions

A rigorous study of the behavior of a wide coaxial injection band can be made only by calculating numerical solutions of Eq. (4) with the boundary conditions given in Eqs. (8), (9a)–(9c), (10a), (10b). However, it is possible to use an approach traditional in chromatography in order simply to derive approximate estimates of the behavior of such a band during its migration along the column. The problem has been studied first by Knox and Parcher [26] in linear liquid chromatography with an injection band which was narrow compared to the column diameter (see the boundary condition used by Eon [4] and described in the discussion leading to Eqs. (12a) and (12b)). We now generalize this approach to the case of a wide injection band. Under nonlinear conditions, only qualitative results may be obtained, however.

Elution under infinite column diameter condition is typical of the early applications of analytical column chromatography. With on-column syringe injection, the injected band was narrow in the radial dimension and short. The band dispersed too slowly in the radial direction for the concentration to reach a finite value at the column wall before the band leaves the column. The advantage of this practice was that packed columns (especially those prepared by a dry packing method) tended to have a much lower efficiency close to their wall than in their center (in dry packing, there is a radial segregation of particle size, the larger particles tending to concentrate close to the column wall [27]). If the band does not get close to the wall, it remains in a region of the packing where the efficiency is high or reasonable. The radial width of the injected band, R_{inj} the column aspect ratio, i.e., the ratio $\Phi = L/R$, and the radial dispersion coefficient, D_r, are assumed to be sufficiently small to meet the requirement of no wall interference.

A reasonable estimate of the radius, R'_z, of the band at the position z during its migration along the column is obtained by stating that the variance of the band in the radial direction is equal to the sum of the radial variance of the injected band and of the variance increase during the band migration along the column

$$\sigma_r^2 = \frac{R_{inj}^2}{3} + H_r z = \frac{R_{inj}^2}{3} + 2 \cdot \frac{Lz}{Pe_r} \tag{15}$$

In writing Eq. (15), it was assumed that the axial cross-section of the injection band profile is a rectangle of width $w = 2R_{inj}$ hence second moment $M_2 = w^2/12 = R_{inj}^2/3$. The column is operated under infinite column diameter conditions as long as the radial width of the band (i.e., $4\sigma_r$) is less than the column diameter (a condition supported by the calculations of Eon [4] discussed in Section 2.4), i.e.,

$$4\sigma_r \leq 2R \tag{16a}$$

$$\frac{4R_{inj}^2}{3} + 8 \cdot \frac{Lz}{Pe_r} \leq R^2 \tag{16b}$$

and, at the end of the column (i.e., for $z = L$):

$$\frac{4}{3} \cdot \left(\frac{R_{inj}}{R}\right)^2 + \frac{8}{Pe_r} \cdot \left(\frac{L}{R}\right)^2 \leq 1 \tag{16c}$$

$$\frac{R_{inj}}{R} \leq \sqrt{0.75\left[1 - \left(\frac{L}{R}\right)^2 \cdot \frac{8}{Pe_r}\right]} \tag{16d}$$

As will be made clear by the results of the calculations detailed later, it is difficult to achieve sets of experimental conditions in preparative chromatography which do not fulfil Eq. (16c). For example, typical (see later discussion) values of Pe_r and L/R would be 10 000 and 3, respectively; Eq. (16c) would be satisfied for $R_{inj}/R \leq 0.86$. Note, however, that Eq. (16c) overestimates the band width since the largest possible value of R_{inj}/R given by Eq. (16d) is 0.866 (for $Pe_r = \infty$).

A better estimate of the condition for infinite column diameter behavior can be obtained by considering the evolution through radial diffusion of the profile of a concentration step of width $2R_{inj}$ ending in vertical discontinuities at both ends, at time $t = 0$. We assume that the height of the concentration step remains constant because the amount of solute involved in the radial diffusion is small. Then, at time $t = L/u$, the profile is an erf function with a

variance $\sigma_r'^2 = 2L^2/Pe_r$ and an inflection point located at R_{inj}. The practical width of the band is $2(R_{inj} + 2\sigma_r')$. The condition for infinite column diameter is now

$$R_{inj} + 2\sigma_r' \leq R \tag{17a}$$

$$\frac{R_{inj}}{R} \leq 1 - 2\frac{L}{R}\sqrt{\frac{2}{Pe_r}} \tag{17b}$$

For the typical values of Pe_r and L/R used above (10 000 and 3, respectively), we find now that the relative width of the central injection should be no more than 0.915.

Obviously, when the injection radius becomes negligible, Eq. (17b) reduces to the condition of Knox and Parcher [26]:

$$L \leq \frac{d_c^2}{16H_r} \tag{17c}$$

Knox and Parcher had assumed that the axial HETP was equal to $0.15d_p$. This value is in agreement with the results of recent determinations by PFG NMR [10–12].

3. Results and discussion

The most important parameter in this work is the ratio of the axial and transverse dispersion coefficients. They are related to the axial and transverse HETP, respectively (Eqs. (2) and (5)), and to the mobile phase velocity through the Giddings [22] equation by the following relationships:

$$D_a = \frac{uH_a}{2} = \frac{u}{2}\cdot\frac{\partial\sigma_a^2}{\partial z} = \frac{ud_p}{2}\cdot\left(\frac{2\gamma}{\nu} + \sum_i \frac{2\lambda_i}{1+\omega_i\nu^{-x}} + C\nu\right) \tag{18a}$$

$$D_r = \frac{uH_t}{2} = \frac{u}{2}\cdot\frac{\partial\sigma_t^2}{\partial z} = \frac{ud_p}{2}\cdot\left(\frac{2\gamma}{\nu} + D\right) \tag{18b}$$

with D_m, molar diffusivity, d_p, average particle size, $\nu = ud_p/D_m$, reduced velocity (or particle Peclet number), and γ tortuosity of the column bed. x is usually assumed to be equal to unity. C and D are numerical coefficients which depend on the experimental conditions (e.g., particle size, retention factor). Knox and Saleem [23] proposed to replace the intermediate term $[\Sigma_i (2\lambda_i)/(1+\omega_i\nu^{-x}]$ by a simpler expression $(A\nu^{0.33})$ which is numerically equivalent in the range of velocities of practical interest. This empirical equation is often preferred for the sake of its simplicity. The experimental validity of Eqs. (18a) and (18b) has been established by direct measurements [24] and by PFG NMR determinations of the dispersion in chromatographic columns [10–12].

The experimental results obtained by Eon [4], Baumeister et al. [10] and Tallarek et al. [11,12] show that the radial [4] or transverse [10–12] dispersion coefficient is usually much lower than the apparent axial dispersion coefficient. At typical mobile phase velocities used in preparative liquid chromatography (i.e., for values of the reduced velocity between 4 and 20), the ratio D_a/D_r is almost always larger than 3, often between 5 and 10 and sometimes (at high velocities) even somewhat larger than that [4,10–12]. The reason for the considerable difference between these two dispersion coefficients is explained by the relatively large contribution of the mass transfer resistance to the apparent axial diffusion coefficient while this contribution has no effect on the transverse coefficient. The mass transfer resistance contribution increases rapidly with increasing flow velocity. For example, in the case of the data published by Baumeister et al. [10], the ratio D_a/D_r becomes equal to 2 for a reduced velocity approximately equal to 2. For a reduced velocity of 3.5, it is 3.1. In the case of the data published by Tallarek and co-workers, the ratio D_a/D_r is equal to 2 and 10 for values of the reduced velocity of approximately 2.5 and 22, respectively. Calculations have been made for values of the ratio $D_a/D_r = Pe_r/Pe_a$ (Eqs. (6d) and (6e)) between 5 and 20 although most calculations were made with a ratio of 5. In view of the previous discussion, these values appear as quite realistic.

Since D_r is much smaller than D_a, Pe_r is much larger than Pe_a (cf. Eqs. (6d), (6e), (7)). At the large values of the radial Peclet number which are achieved at high mobile phase velocities, radial dispersion becomes slow and the radial width of the band increases moderately during its elution. As a matter of fact, such a phenomenon is clearly seen on the developed chromatoplates obtained in thin-layer

chromatography (TLC), especially when these plates are made with coarse particles and the velocity of the mobile phase is high [25]. Such spots are elliptical, with the axis parallel to the direction of development much longer than the perpendicular axis, and have an aspect ratio which is often in the range of 2 to 3 (the aspect ratio of a TLC spot is equal to the average value of the ratio D_a/D_r during the development). Still the range of mobile phase velocity achieved during the development of TLC plates is well below the one reached in column chromatography, accounting for a ratio Pe_r/Pe_a closer to unity than in column chromatography.

3.1. Typical band profile

In order to illustrate more clearly the following discussion, we show the changes in band profiles obtained by changing one parameter at a time. Fig. 2, the reference figure for these comparisons, was calculated with $Pe_a = 2000$ (i.e., a column efficiency of 1000 theoretical plates) and $Pe_r = 10\,000$, corresponding to a ratio $D_a/D_r = 5$, typical of those observed in current practice (see above) [10–12]. The column length was $L = 15$ cm and its diameter, $2R = 5$ cm. The column dimensions are typical of the rather fat columns actually used in preparative chromatography. The equilibrium isotherm is given by the Langmuir equation (Eq. (3), with $a = 12.0$, $b = 0.024$ and $F = 0.45$). In this work, the loading factor, $L_f = nb/(\epsilon SLk_0')$ (n number of moles of compound injected, S, column cross-sectional area), is calculated after the amount injected, the specific saturation capacity of the stationary phase, and the amount of this phase in a column of length L and diameter R_{inj}. This loading factor is kept at $L_f = 0.10$. This means that the classical loading factor is $0.10 \cdot (R_{inj}/R)^2$ and varies according to R_{inj}. This choice was made because it seemed more realistic to keep constant the density of feed across the column inlet rather than the amount of feed injected. In the case of Fig. 2, $R_{inj}/R = 0.50$, hence the injection covers only a quarter of the cross-sectional surface area of the column and the operational loading factor is 0.025.

The profile is illustrated in Fig. 2, with Fig. 2a showing a false three-dimensional plot with the product of the concentration and the second Langmuir coefficient (Eq. (3)) along the vertical axis (bC), the (normalized) retention time ($\tau = t_R/t_0$) along the abscissa axis, and the (normalized) radial position along the ordinate axis ($\rho = r/R$). The retention factor is 5.4. At injection, the feed pulse had a reduced radius of 0.50. Fig. 2b Fig. 2c Fig. 2d show a series of cuts of the band profile in Fig. 2a by the family of planes of equations $X = \tau = t/t_0 = \text{const}$, $Y = \rho = r/R = \text{const}$, and $Z = bC = \text{const}$, respectively.

The profile obtained results from a combination of two phenomena. First, as under conventional conditions, the band broadens in the axial direction because of overloading and its axial profile at any radial position in the central area corresponds to a conventional Langmuirian profile. This is illustrated by profile No. 5 in Fig. 2b. Second, the band broaden radially, by diffusion. This is illustrated by the profiles in Fig. 2c which are made of two symmetrical, rather steep error functions. Note, however, that the radial sections of the three-dimensional band profiles are narrower in the steep region in front of the ridge (corresponding to the self-sharpening front observed in conventional chromatography (one spatial dimension) than in the tail part (the diffuse rear). This is because the high concentrations move faster than the low concentrations (with a langmuirian isotherm). The concentration which diffuse radially from the high concentration ridge to form the lateral part of the band are low, hence move more slowly than the center of the band front, and they tend to be left behind. This explains the shape of the isoconcentration contours (Fig. 2d). They are straight in front of the band where they pile-up closely. They broaden in the rear and their spacing increases.

3.2. Influence of the main experimental parameters

The influences of the column efficiency (i.e., Pe_a) and of the sample size (or loading factor) on the band profiles are already well known [1] and will not be discussed again here. For the sake of simplicity, the whole discussion will be limited to the case in which the column efficiency is 1000 theoretical plates ($Pe_a = 2000$) and the loading factor over the fraction of the cross-sectional area which is loaded with feed is 10%. Since the loading factor is estimated for the amount of stationary phase in the column of length L and radius R_{inj} the stationary phase at the center of

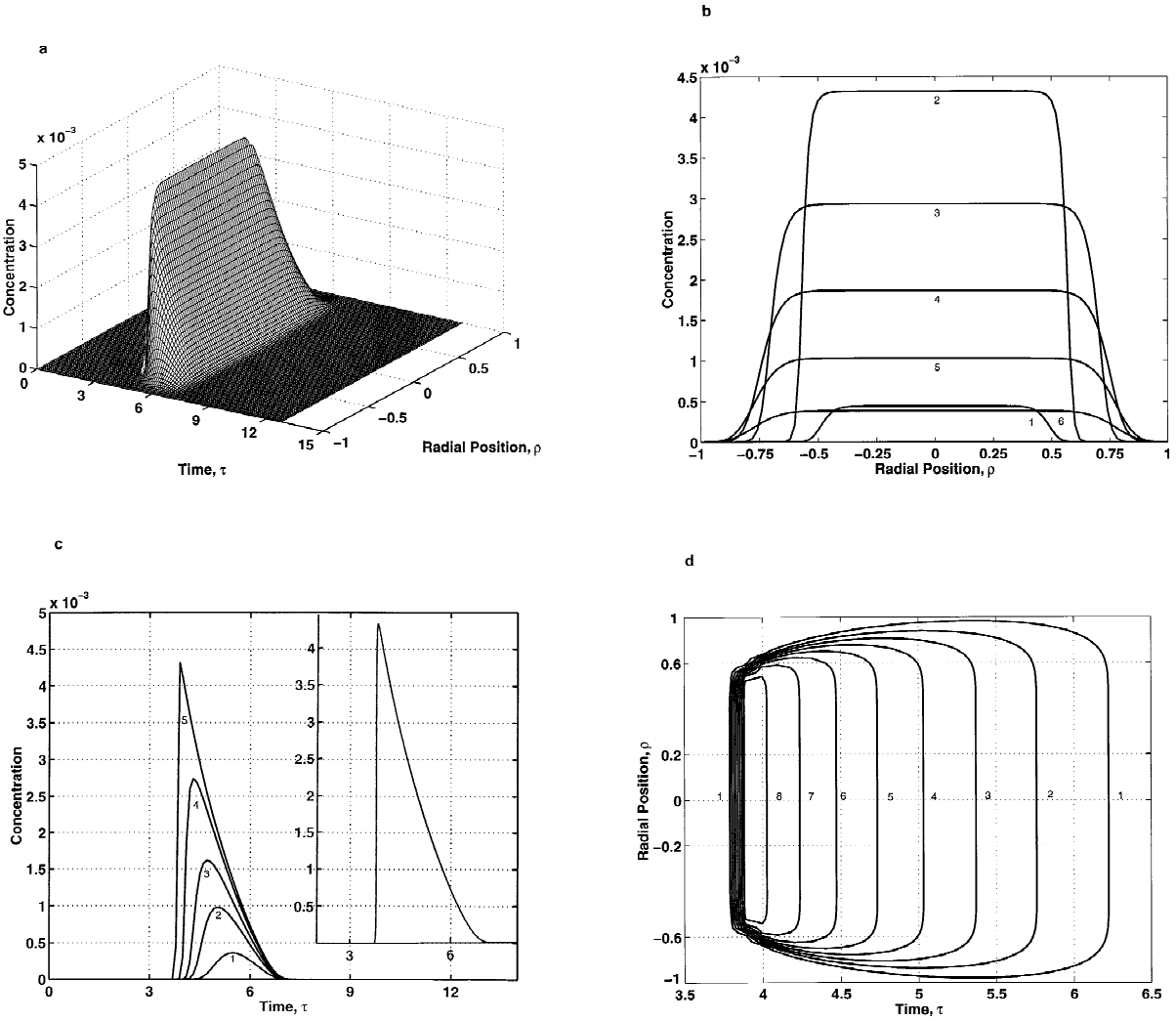

Fig. 2. Elution of a band of relative radius $R_{inj}/R=0.50$, covering a fractional area of 25% of the column cross-section. This is the reference figure for further comparisons. Local loading factor, 10%; column length, 15 cm; aspect ratio, 3; $Pe_a=2000$; $Pe_r=10\,000$. Mobile phase linear velocity, $u=0.123$ cm/s. $t_0=121.8$ s. (a) Three-dimensional representation of the band profile in a τ, ρ, bC space. (b) Plot of the concentration versus the radial position, ρ, at constant values of the reduced elution time (i.e., sections of the surface in (a) by planes $X=t/t_0=\tau=$const). Values of τ: curve 1, 3.79; curve 2, 3.89; curve 3, 4.51; curve 4, 5.12; curve 5, 5.73; curve 6, 6.35. (c) Plots of the concentration versus the elution time, τ, at constant value of $\rho=r/R$ (i.e., sections of the surface in (a) by planes $Y=\rho=$const). Values of ρ: curve 1, 0.80; curve 2, 0.74; curve 3, 0.70; curve 4, 0.64; curve 5, 0.00. Inset: elution band profile obtained with the equilibrium–dispersive model, in the case of a one-spacial-dimension column, with $L_f=0.10$; $Pe_a=2000$; $L=15$ cm. (d) Plot of the radial position, ρ, versus the elution time, τ, at constant values of the concentration (i.e., sections of the surface in (a) by planes $Z=bC=$const). Values of C: curve 1, 0.005; curve 2, 0.025; curve 3, 0.050; curve 4, 0.075; curve 5, 0.100; curve 6, 0.125; curve 7, 0.150; curve 8, 0.175.

the column is operated under constant degree of overloading and the axial band profile at $\rho=0$ will remain essentially unaffected by a change in R_{inj} unless the injection band becomes very narrow (see later). This remark affords a method of validation of the new program. In Fig. 2c, the band profile obtained at $\rho=0$ (profile No. 5) is compared to the profile calculated with the conventional backward–forward scheme of numerical calculations of band profiles in the equilibrium–dispersive model with

one spatial dimension [1] for $Pe_a = 2000$, $L_f = 0.10$, and $L = 15$ cm. These two profiles overlay nearly exactly. The only minor differences are the result of a larger mesh size of the calculation grid, required to keep a reasonable run time for the calculations.

We focus this discussion on the other important parameters, the radial dispersion coefficient, the column length (at constant column diameter), and the relative ratio, $\rho_{inj} = R_{inj}/R_c$ (Eqs. (9a) and (9b)) of the injection band and the column diameters.

3.2.1. Influence of the radial dispersion coefficient

Figs. 3 and 4 show the band profiles obtained for two other values of the radial Peclet number, 5000 and 20 000, corresponding to ratios D_a/D_r of 2.5 and 10, respectively. Together with Fig. 2, these figures complete a series covering the practical range of the ratio D_a/D_r encountered in practical applications (see earlier discussion). The extent of radial dispersion of the band increases with decreasing value of Pe_r, as illustrated by the planar sections and with $bC = \text{const}$ (Figs. 2b, 3b, 4b). The sections in Fig. 2b were made at the same values of τ (see captions). The concentration heights are the same in the center of the bands (horizontal part of the profiles) but the diffuse parts on the side increase in relative width with decreasing value of Pe_r.

In none of these three cases, however, does the concentration become significantly different from 0 close to the column wall (see Fig. 3b, for the lowest value of Pe_r). In practice, an injected band coaxial with the column and filling 25% of the cross-sectional area will be eluted under conditions of infinite-diameter column [26].

3.2.2. Influence of the column length

When the column length increases at constant mobile phase velocity, the retention time increases but $\tau = t_R/t_0$ remains constant. The band profiles change at constant value of the other parameters, however, because the time spent by the band inside the column increases, hence the extent of radial dispersion that it undergoes increases also. This effect is illustrated by a comparison between Figs. 2 and 5, which shows the band profile obtained with a column of length 30 cm (and the same diameter), hence an aspect ratio of 6. The extent of radial dispersion is more important with the longer column because the velocity has been kept constant, hence the band spends twice as long in the 30 cm long column as in the 15 cm long one. Although the

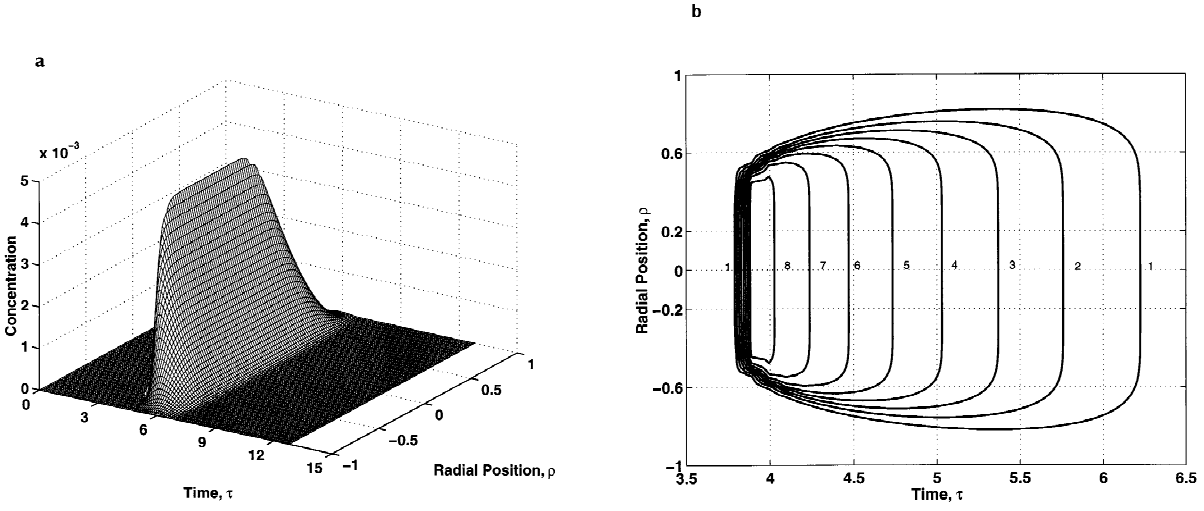

Fig. 3. Same as Fig. 2, except $Pe_r = 5000$. Elution profile of an injected band covering a fractional area of 25% of the column cross-section. Local loading factor, 10%; column length, 15 cm; aspect ratio, 3; $Pe_a = 2000$. (a) Three-dimensional representation of the band profile. (b) Sections of the surface in (a) by planes $bC = \text{const}$. Values of C: curve 1, 0.005; curve 2, 0.025; curve 3, 0.050; curve 4, 0.075; curve 5, 0.100; curve 6, 0.125; curve 7, 0.150; curve 8, 0.175.

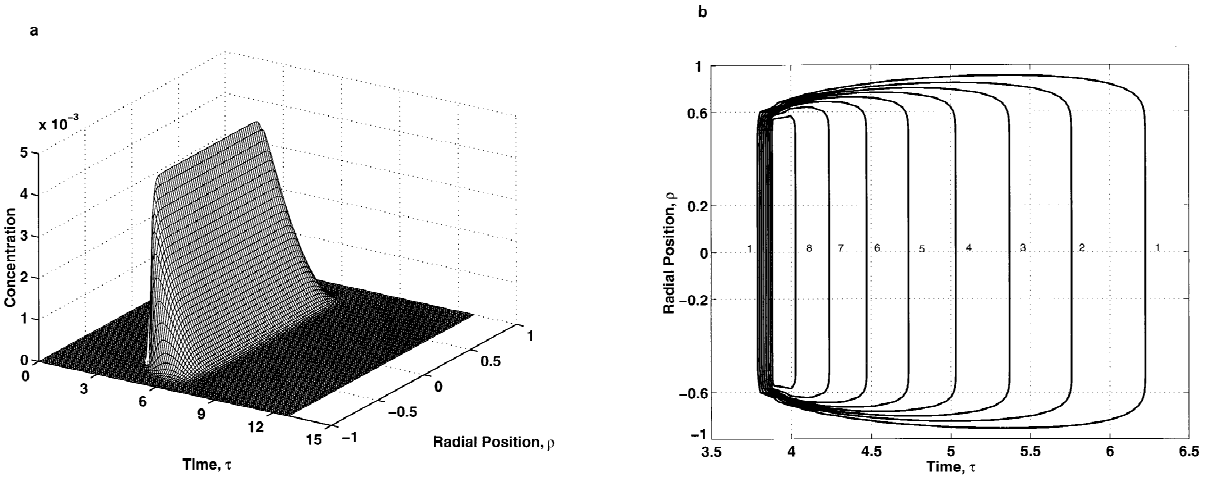

Fig. 4. Same as Fig. 2, except $Pe_r = 20\,000$. Elution profile of an injected band covering a fractional area of 25% of the column cross-section. Local loading factor, 10%; column length, 15 cm; aspect ratio, 3; $Pe_a = 2000$. (a) Three-dimensional representation of the band profile. (b) Sections of the surface in (a) by planes $bC = \text{const.}$ Values of C: curve 1, 0.005; curve 2, 0.025; curve 3, 0.050; curve 4, 0.075; curve 5, 0.100; curve 6, 0.125; curve 7, 0.150; curve 8, 0.175.

concentration remains low at the wall (ca. 0.011 or 6% of the band maximum), it is no longer completely negligible. The band might experience some significant deformation if the wall region has properties which are markedly different from those of the core [2–9].

3.2.3. Influence of the radial width of the injection band

Figs. 6 and 7 show the band profiles obtained with two other values of the radial width of the injection band, $\rho_{inj} = 0.70$ (fraction of the cross-section area, 50%) and 0.90 (fraction of the cross-

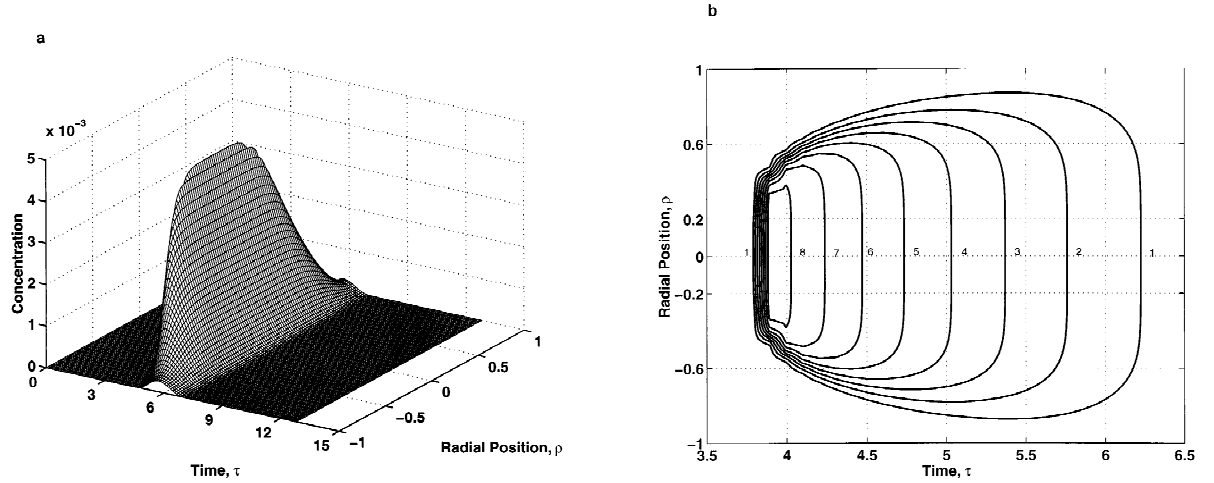

Fig. 5. Same as Fig. 2, except $L = 30$ cm. Elution profile of an injected band covering a fractional area of 25% of the column cross-section. Local loading factor 10%; column radius, 5 cm; aspect ratio, 6; $Pe_a = 2000$; $Pe_r = 10\,000$. (a) Three-dimensional representation of the band profile. (b) Sections of the surface in (a) by planes $bC = \text{const.}$ Values of C: curve 1, 0.005; curve 2, 0.025; curve 3, 0.050; curve 4, 0.075; curve 5, 0.100; curve 6, 0.125; curve 7, 0.150; curve 8, 0.175.

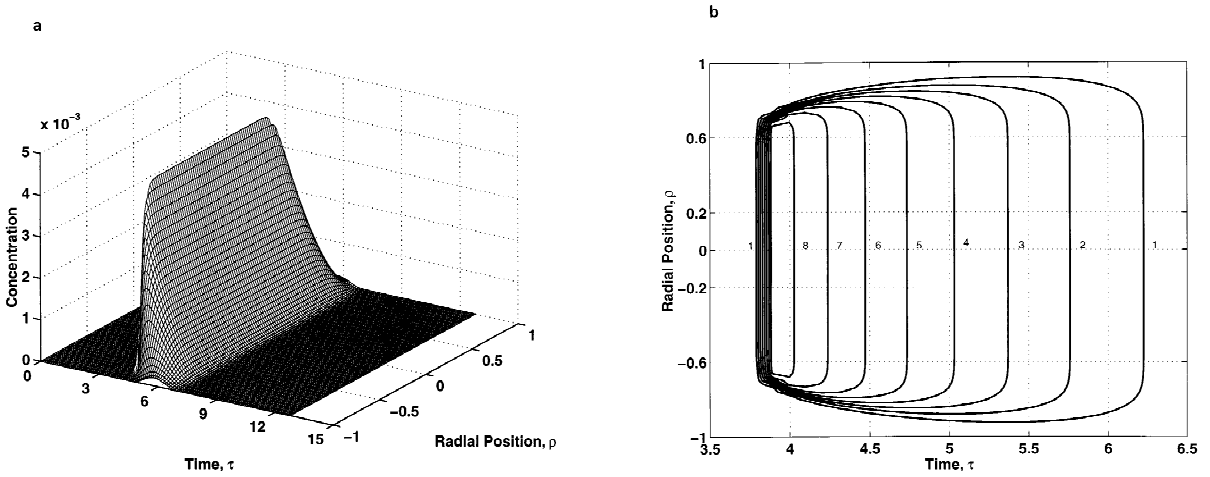

Fig. 6. Same as Fig. 2, except radial width of the injection band, $R_{inj}/R=0.70$. Local loading factor, 10%; column length, 15 cm; aspect ratio, 3; $Pe_a=2000$; $Pe_r=10\,000$. (a) Three-dimensional representation of the band profile. (b) Sections of the surface in (a) by planes $bC=$const. Values of C: curve 1, 0.005; curve 2, 0.025; curve 3, 0.050; curve 4, 0.075; curve 5, 0.100; curve 6, 0.125; curve 7, 0.150; curve 8, 0.175.

section area, 80%), respectively. Compared to the profiles in Fig. 2, the profiles widen with increasing radial width of injection (see also the figures showing the contours in the three planar directions). For large widths of the injection band, i.e., with ρ equal to or larger than 0.75, the concentration at elution becomes significantly different from 0 at the wall. This effect is most notable in Fig. 7 ($\rho_{inj}=0.90$). Already in Fig. 6, however, the concentration exceeds slightly 10% of the maximum peak concentration at $\rho_{inj}=0.90$ (Fig. 7b, τ between 5 and 5.5). Obviously, the effect depends also, and rather strong-

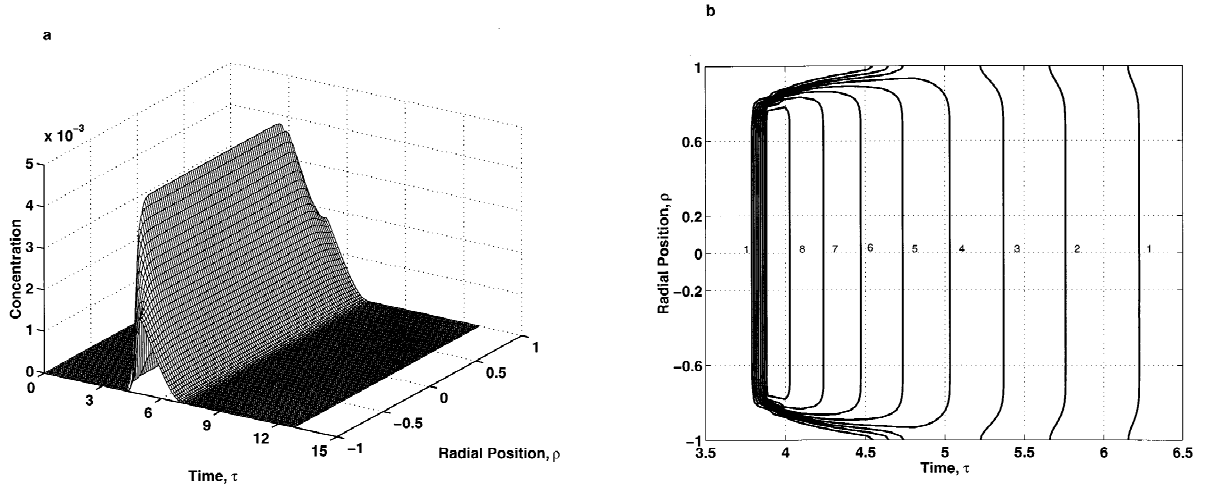

Fig. 7. Same as Fig. 2, except radial width of the injection band, $R_{inj}/R=0.90$. Local loading factor, 10%; column length, 15 cm; aspect ratio, 3; $Pe_a=2000$; $Pe_r=10\,000$. (a) Three-dimensional representation of the band profile. (b) Sections of the surface in (a) by planes $bC=$const. Values of C: curve 1, 0.005; curve 2, 0.025; curve 3, 0.050; curve 4, 0.075; curve 5, 0.100; curve 6, 0.125; curve 7, 0.150; curve 8, 0.175.

ly, on the value of the radial dispersion coefficient (cf. Figs. 2d, 3b and 4b).

The cross-sections of the band profile (Figs. 2a, 6a and 7a) made in the direction of the radial position, by planes $\rho = \text{const}$, give curves which are qualitatively similar to the plots of the peak height versus the radial position or radial concentration profiles reported by Eon [4], provided one takes into account the effect of a finite width of the injection band on these distributions. For normalization purpose, this author defined a critical column length, L_1, as the length for which the peak variance is one-quarter of the column radius (Eqs. (12a) and (12b)). In the particular case of our figures, the value of L_1 is 88 cm (with $Pe_r = 10\,000$). This is why the concentration of the elution bands is different from 0 close to the column wall only in the cases of very wide injection pulses (Fig. 6).

A quantitative comparison between the curves in Figs. 2b, 3b, 4b, 5b, 6b and 7b shows, however, that the conventional approach discussed in connection with the derivation of Eqs. (16a)–(16d), (17a)–(17c) is simplistic and does not provide a satisfactory solution under nonlinear conditions. Note that, in nonlinear chromatography, the rule of variance additivity is not valid because the convolution is shift-variant [28]. Thus, Eq. (17b) is based on a model of the radial concentration distribution given by two errors functions, one on each side of the band, located at $\rho = \rho_{inj}$ and having a constant standard deviation. It predicts that, if the injection diameter, ρ_{inj} is less than 0.91, the concentration at the wall will be negligible. We see in Fig. 7d that the radial distribution of the concentration is well predicted by an error function on each side of the band. However, the location of the inflection point of the error function depends on the location of the section. It moves closer to the wall with increasing retention time while the standard deviation increases.

3.3. Radial band broadening during elution under conditions of infinite column diameter

Figs. 2–7 show the elution profiles corresponding to relatively wide injection bands, wide enough for the concentration to reach values which are not always entirely negligible close to the column wall (e.g., Fig. 5). However, the band profile remains essentially unaffected by the presence of the column wall and, in this sense, these bands can be considered as eluted under conditions of infinite column diameter. In order to illustrate an actual case, as it was achieved with on-column, central syringe injection, a calculation has been made with a value of $\rho_{inj} = 0.010$, corresponding to an injection covering only 0.01% of the inlet cross-sectional area of the column while the other parameters remain the same as for Fig. 2. The sample size corresponds to a loading factor equal to 10%, based on the injection area. In other words, the actual loading factor of the column is 0.001% (a tiny amount, corresponding to an analytical size injection, if it were not for its most heterogeneous distribution over the inlet cross-section of the column). A high concentration and a high degree of non-linear behavior is achieved at the column center but dispersion proceeds in both the axial and radial directions. When the local concentration has decreased more than ten-fold, the behavior tends to become linear and all concentrations move at the velocity $u/(1+Fa)$.

The results of the calculation are shown in Fig. 8. Note that the elution profile of the band (see especially the section by the vertical plane $\rho = 0$), exhibits a steep front (shock layer) caused by the nonlinear behavior due to local overload and a Langmuir isotherm. The high concentrations migrate faster than the low ones and the front is self-sharpening. Note also that the isoconcentration profiles at low concentrations (Fig. 8) have the shape of an egg, with the small end around the front shock layer. This is again explained by the fact that high concentrations move faster than low ones. On the side of the band, the concentrations are lower than in its center, and they tend to be left behind. Obviously, an increase in the value of the axial or radial Peclet number would result in a less important axial and radial spreading of the band. The band would become less dilute; shorter along the time axis, narrower and taller. However, it is clear that, for the value of the radial Peclet number used, the concentration at the wall is entirely negligible. This band profile illustrates band migration under the infinite column diameter effect. It never experiences any perturbation in the properties of the packed bed due to the proximity of the column wall. Because the radial dispersion is so slow compared to the migra-

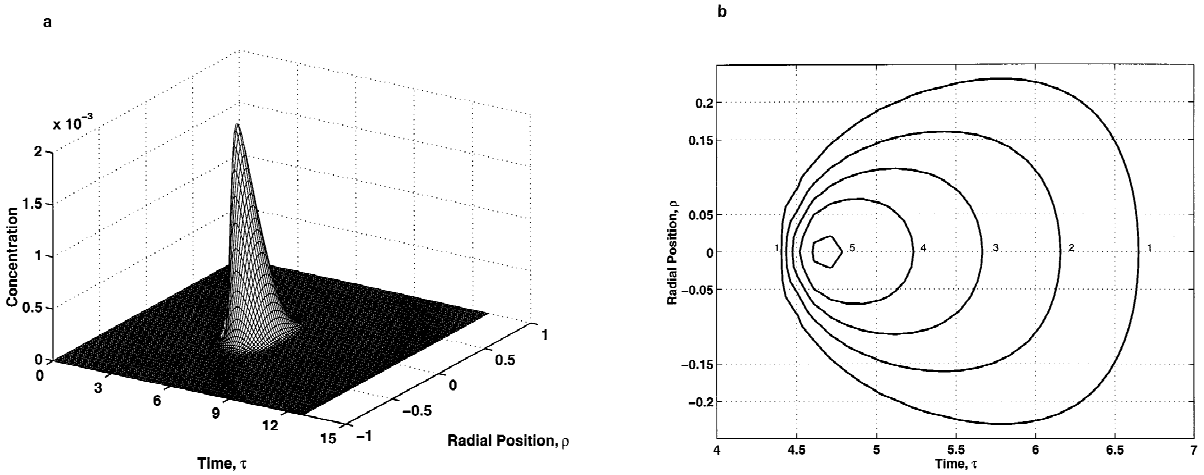

Fig. 8. Same as Fig. 2, except radial width of the injection band, $R_{inj}/R=0.010$. Elution profile of an injected band covering a fractional area of 0.01% of the column cross-section. Local loading factor, 10%; column length, 15 cm; aspect ratio, 3; $Pe_a=2000$; $Pe_r=10\,000$. (a) Three-dimensional representation of the band profile. (b) Sections of the surface in (a) by planes $bC=$const. Values of C: curve 1, 0.005; curve 2, 0.020; curve 3, 0.040; curve 4, 0.060; curve 5, 0.080.

tion of the band along the column, an overloaded elution profile is achieved in spite of the very low global loading factor of 0.001%. This illustrates one of the practical drawbacks of central injection for analytical applications.

4. Conclusions

In most columns, the bed is heterogeneous close to the column wall. In such cases, the column efficiency appears poor because the band moves at different velocities in the region close to the wall and in the core region [6–9]. Then, it becomes warped and the apparent efficiency is lower than the local efficiency [10–12]. The core part of the packing is rather homogeneous and exhibits a higher local efficiency than the wall region [8,9]. The deleterious dispersive effects of the difference between the convective and dispersive properties of the core and the wall regions could be avoided by using only the core part of the column. This could be achieved by distributing the feed injected over a central region of the column. During its elution, the injected band would not migrate through the wall region and would not be warped. This procedure would afford less dispersed, better separated component bands, hence a gain in recovery yield or in production rate if a larger sample would be injected to keep the resolution constant. The actual loading factor achieved by reducing the area covered by the injected band at constant sample density decreases, however. Whether the balance between the two effects, production gain achieved through better efficiency with a centrally injected band and loss caused by the reduction of the useful section area of the column will be positive is unclear and depends much on the degree of homogeneity of the packing achieved in a specific case.

The implementation of the concept of a column with an infinite diameter was originally suggested by Knox and Parcher [26] for analytical columns. It is not compatible with valve injection. It could be effectively reduced to practice only for the large scale preparative columns used in industrial separations. The importance of the wall region in such columns is unknown as well as the extent of the amount of dispersion that it might cause. The only published study suggests that the wall region is thick and, at least in some cases, causes significant loss of performance. In such a case, the process could be interesting mainly when high purity products are required because a high resolution is needed. Then, the gain in production achieved by avoiding the use of the wall region may be worth the cost. This includes the reduced throughput and the design and construction of a special coaxial inlet to allow a

sheet of mobile phase along the wall while the feed is centrally injected.

5. Symbols

A Courant number of the problem (Eqs. (14a) and (14b))
a Numerical coefficient in the Langmuir isotherm (Eq. (3))
b Numerical coefficient in the Langmuir isotherm (Eq. (3))
C Solute concentration in the mobile phase (Eq. (3))
C Numerical coefficient (Eqs. (18a) and (18b), Giddings plate height equation)
C_0 Concentration of the injected sample (Eqs. (9a)–(9c))
D Numerical coefficient (Eqs. (18a) and (18b), Giddings plate height equation)
D_a Apparent axial dispersion coefficient (Eq. (1))
D_m Molar diffusivity (Eqs. (18a) and (18b))
D_r Radial dispersion coefficient (Eq. (4))
d_p Average particle size (Eqs. (12a) and (12b))
F Phase ratio $[F=(1-\varepsilon)/\varepsilon]$ (Eq. (1))
F_v Mobile phase flow-rate (Eqs. (9a)–(9c))
H_a HETP of the column in the axial direction (Eq. (2))
H_r Radial plate height (Eq. (5))
L Column length (Eqs. (6a)–(6f))
L_1 Length for which the peak variance in the radial direction is one-quarter of the column radius (Eqs. (12a) and (12b))
L_f Loading factor
L_f Loading factor density along the column axis (Eqs. (9a)–(9c))
n Injected amount (Eqs. (9a)–(9c))
Pe_a Axial column Peclet number (Eqs. (6a)–(6f))
Pe_r Radial column Peclet number (Eqs. (6a)–(6f))
q Solute concentration in the stationary phase (Eq. (1))
r Distance from the column axis (Eq. (4))
R Column radius (Eqs. (6a)–(6f))
R_{inj} Radius of the injected pulse (Eqs. (9a)–(9c))
S Column cross-sectional area
t Time (Eq. (1))
t_p Width of the rectangular pulse of injected sample (Eqs. (9a)–(9c))
u Mobile phase flow velocity (Eq. (1))
x Coefficient in the general plate height equation (usually assumed to be equal to unity) (Eqs. (18a) and (18b))
z Distance along the column (Eq. (1))

5.1. Greek characters

χ Reduced axial position (Eqs. (6a)–(6f))
γ Tortuosity of the column bed (Eqs. (18a) and (18b), Giddings plate height equation)
δt Time increment in the numerical calculation (Eqs. (14a) and (14b))
δz Length increment in the numerical calculation (Eqs. (14a) and (14b))
ε Total column porosity (Eq. (1))
λ_i Numerical coefficient (Eqs. (18a) and (18b), Giddings plate height equation)
ν Particle Peclet number or reduced velocity (Eqs. (18a) and (18b))
ρ Reduced column radius (Eqs. (6a)–(6f))
σ_r^2 Variance of the band in the radial direction (Eq. (15))
τ Reduced time (Eqs. (6a)–(6f))
Φ Column aspect ratio (Eqs. (6a)–(6f))
ω_i Numerical coefficient (Eqs. (18a) and (18b), Giddings plate height equation)

Acknowledgements

This work has been supported in part by Grant DE-FG05-88ER13859 of the US Department of Energy and by the cooperative agreement between the University of Tennessee and the Oak Ridge National Laboratory. We acknowledge the support of our computational effort by the University of Tennessee Computing Center.

References

[1] G. Guiochon, S. Golshan Shirazi, A.M. Katti, Fundamentals of Preparative and Nonlinear Chromatography, Academic Press, Boston, MA, 1994.
[2] D.S. Horne, J.H. Knox, L. McLaren, Sep. Sci. 1 (1966) 531.
[3] J.H. Knox, G.R. Laird, P.A. Raven, J. Chromatogr. 122 (1976) 129.
[4] C. Eon, J. Chromatogr. 149 (1978) 29.

[5] J.E. Baur, E.W. Kristensen, R.M. Wightman, Anal. Chem. 60 (1988) 2338.
[6] T. Farkas, J.Q. Chambers, G. Guiochon, J. Chromatogr. A 679 (1994) 231.
[7] T. Farkas, M.J. Sepaniak, G. Guiochon, J. Chromatogr. A 740 (1996) 169.
[8] T. Farkas, M.J. Sepaniak, G. Guiochon, AIChE J. 43 (1997) 1964.
[9] T. Farkas, G. Guiochon, Anal. Chem. 69 (1997) 4592.
[10] E. Baumeister, U. Klose, K. Albert, E. Bayer, G. Guiochon, J. Chromatogr. A 694 (1995) 321.
[11] U. Tallarek, K. Albert, E. Bayer, G. Guiochon, AIChE J. 42 (1996) 3041.
[12] U. Tallarek, E. Bayer, G. Guiochon, J. Am. Chem. Soc. 120 (1998) 1494.
[13] U. Tallarek, E. Bayer, G. Guiochon, AIChE J., in press.
[14] G. Guiochon, T. Farkas, H. Guan-Sajonz, J.-H. Koh, M. Sarker, B.J. Stanley, T. Yun, J. Chromatogr. A 762 (1997) 83.
[15] K. Mihlbachler, A. Seidel-Morgenstern, J. Tomas and G. Guiochon, J. Chromatogr. A, submitted for publication.
[16] G. Guiochon, E. Drum, D. Cherrak, J. Chromatogr. A, submitted for publication.
[17] T. Yun, G. Guiochon, J. Chromatogr. A 734 (1996) 97.
[18] J. Zhang, G. Guiochon, in preparation.
[19] B. Stanley, M. Sarker, G. Guiochon, J. Chromatogr. A 741 (1996) 175.
[20] A. Klinkenberg, H.J. Krajenbrink, H.A. Lauwerier, Ind. Eng,. Chem. (Process Kinetics) 45 (1953) 1202.
[21] D.J. Gunn, Chem. Eng. Sci. 35 (1980) 2405.
[22] J.C. Giddings, Dynamics of Chromatography, Marcel Dekker, New York, 1965.
[23] J.H. Knox, M. Saleem, J. Chromatogr. Sci. 7 (1969) 614.
[24] P. Magnico, M. Martin, J. Chromatogr. 517 (1990) 31.
[25] F. Geiss, Fundamentals of Thin Layer Chromatography, Hüthig, Heidelberg, 1987.
[26] J.H. Knox, J. Parcher, Anal. Chem. 41 (1969) 1599.
[27] J.C. Giddings, E.N. Fuller, J. Chromatogr. 7 (1962) 255.
[28] E. Dose, G. Guiochon, Anal. Chem. 61 (1990) 1723.